Decanuclear FeIII clusters with hemiacetal ligands: a new{M10(μ3-O)8} cluster core†

J. Mayans,[a] L. Roc,[a] M. Font-Bardia[b] and A. Escuer [*a]

A Departament de Química Inorgànica i Orgànica, Secció Inorgànica and Institute of Nanoscience (IN2UB) and Nanotecnology, Universitat de Barcelona, Martí i Franquès 1-11, Barcelona-08028, Spain.
b Departament de Mineralogia, Cristal·lografia i Dipòsits Minerals and Unitat de Difracció de R-X, Centre Científic i Tecnològic de la Universitat de Barcelona (CCiTUB), Universitat de Barcelona, Solé i Sabarís 1-3, 08028 Barcelona, Spain

albert.escuer@qi.ub.es.(Albert Escuer)

ABSTRACT:

The characterization of a decanuclear FeIII cluster with α-methyl-2-pyridinemethanolate, generated by the hydrolysis of Schiff bases, inspired us to carry out an initial exploration of the direct syntheses of medium nuclearity FeIII clusters starting from aldehydes in methanolic medium. The new complexes exhibit an unprecedented {Fe10(μ3-O)8} cluster core.

Clusters containing oxo-bridged FeIII cations have been widely studied due to their biological relevance as mimics of iron storage proteins or in the search for Single Molecule Magnet (SMM) responses. The oxo bridges between FeIII cations give usually antiferromagnetic interactions that allow low or zero spin ground states. However, high ground spin states, exhibiting slow relaxation of magnetization, can be stabilized for some topologies like Fe4 iron-stars or Fe8 clusters, which are among the earlier and best studied SMM families.1–5

2-(Hydroxymethyl)pyridine (Hhmp) is a classic ligand that has been largely employed in CuII, NiII and MnII,III,IV cluster chemistry (more than 250 entries in the CCDC database) but, in contrast, its reactivity with FeIII is limited to some scarce Fe2, Fe4 , Fe6 , and Fe8 and one Fe9 complexes6–10 mainly reported by Christou and Brechin, while polynuclear derivatives of the chiral related ligand, HMehpm (α-methyl-2-pyridinemethanol), are unprecedented in FeIII chemistry.

The condensation reaction between an aldehyde and an amine to produce a Schiff base can be reversed by hydrolysis to give the starting reagents, usually helped by its coordination to polarizing cations, as FeIII is. The metal assisted nucleophilic attack of a methoxide on the carbonyl C-atom of the coordinated aldehyde yields the hemiacetal methoxy(pyridine-2yl)methanolato (MeO-hmp−) ligand. This ligand is chiral, but the reaction is not selective and produces the (R)/(S)-MeOhmp−racemic mixture. This reaction is well known in organic chemistry but in cluster chemistry it has been reported in very few cases by the deliberate or accidental reaction of 2-pyridinecarboxaldehyde and methanol,11–17 due to the breaking of Schiff bases and subsequent reaction of the aldehyde18–20 or due to an unexpected oxidation of Hhmp.21 Noteworthily, coordination of MeO-hmp− to iron cations has been observed only one time in a mononuclear FeII complex and in one mixed FeIIILnIII complex.19,20 The reaction of the neutral L1 Schiff base (obtained by condensation of 2-pyridylaldehyde with 1,2-diphenyl-ethylenediamine, Scheme 1) with ferric nitrate and sodium thiocyanate in methanolic medium allows us to characterize the decanuclear cluster [Fe10(MeO-hmp−)8(μ3-O)6(μ3-OH)2(NO3)6(NCS)2] (1) or [Fe10(MeO-hmp−)8(μ3-O)7(μ3-OH)(NO3)7] (2) in the absence of thiocyanate. The exclusive presence of MeO-hpm− ligands suggests the complete hydrolysis of L1 and further reaction of the aldehyde with the solvent according to Scheme 1. To check this hypothesis, the direct reaction of ferric nitrate, sodium thiocyanate and 2-pyridinecarboxaldehyde in basic methanolic solution was tried, yielding the same complex 1 or complex 2 in the absence of thiocyanate, proving that the aldehyde was the intermediate reagent in the formation of the decanuclear cluster.

In the light of the reproducibility of 1 and 2 by direct syntheses, we explored the direct reaction with several aldehydes that allowed us to characterize the core of the [Fe10(MeO-3Mehmp−)8(μ3-O)4(μ3-OH)4(NO3)8]2+ cluster starting in this case from 3-methyl-2-pyridinecarboxaldehyde. This set of reactions proves for the first time that this synthetic strategy is a convenient way to obtain high nuclearity FeIII clusters. Synthetic details are provided in the ESI.† IR and powder X-ray spectra are shown in Fig. S1 and S2.†

The structures of 1–3 show a common core that consists of ten FeIII cations in an octahedral environment and sixteen bridging O-donors, Fig. 1. Crystallographic details and selected bond distances and angles are summarized in Tables S1–S4.† The core contains eight μ3-O/μ3-OH bridges and eight μ-O bridges which are provided by the O-alcoxo arms from eight MeO-hmp− ligands. The remaining coordination sites are occupied by six nitrato ligands and two thiocyanates for 1 and only mono or bidentate nitrato ligands for 2 and 3.

Four FeIII cations (Fe1, Fe3, Fe5 and Fe7 for 1 and 2 or Fe(1) and symmetry related for 3, Fig. S4†) link two bidentate MeOhmp−ligands each and show a FeN2O4 environment. The MeO-hmp− ligands are chiral but four of them correspond to the (R)-enantiomer and the other four to the (S)-enantiomer. The iron cations linking (R)-ligands show a Δ conformation, whereas the iron cations linking (S)-ligands exhibit a Λ conformation, showing the expected transference of chirality from the ligand to the cation environment, Fig. S5.†

Fe4, Fe8, Fe9 and Fe10 for 1 and 2 or Fe(3) and symmetry related for 3 have a FeO6 environment formed by one O-alcoxo, three μ3-O and one bidentate nitrato ligands, whereas the apical Fe2 and Fe6 cations are linked by two O-alcoxo, two μ3-O, one N-thiocyanate and one monodentate nitrate ligands, resulting in a FeNO5 environment for 1, by one bidentate and two monodentate nitrates for 2 and by two monodentate nitrates for the case of 3, resulting in FeO6 environments, Fig. 2. The inner {Fe10(O)8} core of the clusters is defined in all the cases by μ3-O and μ3-OH donors which are linked by means of a strong H-bond with the monodentate nitrato ligands. The Fe–Npy and Fe–Onitrate bond distances take large values, up to 2.226 Å, whereas the Fe-(μ3-O/OH) distances are much shorter with values reaching 1.85 Å.

The ten FeIII cations determine a rare polyhedron with exclusively triangular faces, which is unprecedented in cluster chemistry. The most common distortion of a cube biaugmented on two opposite faces (the elongated square bipyramid Johnson solid J15) consists of the rotation of the opposite apicated faces to produce the classical gyroelongated square bipyramid (Johnson solid J17), which can be alternatively described as a biaugmented square antiprism, Scheme 2, left.

This regular deltahedron has 16 faces, 24 edges and 10 vertexes with configuration 2 × 34; 8 × 35. The new polyhedron reported in this work is also derived from the J15 polyhedron but distorted by the displacement of two opposite pairs of edges of the central cube in opposite directions, Scheme 2, right. The resulting polyhedron also has 16 faces, 24 edges and 10 vertexes but with configuration 6 × 34; 4 × 36 related by an S4 improper symmetry axis. The {M10(μ3-O)8} inner core, which is shown in Scheme 2, is unprecedented in cluster chemistry and the search in the CCDC database shows that it can only be found as a fragment of two larger Fe14 clusters which have the S4 edge, ESI Fig. S6.† 22,23 The topological analysis with TOPOS24,25 describes the new {M10(μ3-O)8} core as 4,4,6M10-1.

The room temperature χMT product for 1–3 ranges between 12.47 and 14.8 cm3 mol−1 K which is much lower than the expected value for ten isolated FeIII cations (43.75 cm3 mol−1 K), suggesting a very strong antiferromagnetic coupling, Fig. 3. The χMT value decreases continuously upon cooling,

tending to zero at low temperature. The large number of low-lying spin states, partially populated even at low temperature, makes difficult the observation of the χM maxima but for 2, a susceptibility maximum at 6 K was reached, evidencing unambiguously the S = 0 ground state. The size of the cluster and the large number of superexchange pathways exclude the calculation of the J coupling constants and prevent the fit of the experimental data. This drawback has been overtaken by the fact that the interactions mediated by Fe–O–Fe bridges have been widely studied and their strong dependence on the bond angles and on the Fe–O distances has been well established: the antiferromagnetic interaction increases for large bond angles and short distances and empirical expressions to evaluate the magnitude of the superexchange have been proposed by different authors.26–28

Magnetostructural semiempirical correlations (MSCs) have been recently proposed by Christou et al.28 to predict the J values (2J Hamiltonian, cm−1) for the interactions promoted by Fe–O–Fe bridges as a function of the mean Fe–O distances and the corresponding bond angle, according to the expression:

$$J = 1.23 \times 10^{9} \cdot (-0.12 + 1.57 \cos\phi + \cos^2\phi) \cdot \exp(-8.99 \cdot r).$$

In our case all the FeIII cations of the inner {Fe10(μ3-O)8} core are linked among them by 16 Fe–O–Fe bridges with bond angles comprised between 129.5° and 121.6° and short Fe–Odistances that induce strong AF interactions. The double Fe–O–Fe bridges involving the lower μ3-O angle and the alcoxo donor of the MeO-pym− ligands show angles around 100° and, consequently, a poorly efficient superexchange pathway that does not compete with the interactions promoted by the μ3-O/OH pathways. The MSC calculated J values for the representative complex 1 are shown in Fig. 4, left. These interactions are cooperative and determine the antiparallel alignment of five up and five down local spins which are consequently related among them by a S4 symmetry, Fig. 4 right.

CONCLUSIONS

As a conclusion, we report here the initial exploration of a new synthetic route to obtain high nuclearity FeIII clusters generated by the in situ reaction of pyridylaldehydes with alcohols. The reported Fe10 complexes 1–3 show the largest nuclearity of the FeIII/pyridyl-alcoxo family, exhibiting a new {M10(μ3-O)8} core. The complete study of this new synthesis strategy starting from different counteranions, cations and co-ligands will be reported in a future paper.

158 **ACKNOWLEDGEMENTS**

159

160 Financial support from CICYT, Project CTQ2018-094031-B-100, is acknowledged.

161

REFERENCES

1 G. Christou, D. Gatteschi, D. N. Hendrickson and R. Sessoli, MRS Bull., 2000, 25, 66.

2 D. Gatteschi and R. Sessoli, Angew. Chem., Int. Ed., 2003, 42, 268.

3 A. L. Barra, A. Caneschi, A. Cornia, F. Fabrizi de Biani, D. Gateschi, C. Sangregorio, R. Sessoli and L. Sorace, J. Am. Chem. Soc., 1999, 121, 5302.

4 A. Nava, L. Rigamonti, E. Zangrando, R. Sessoli, W. Wernsdorfer and A. Cornia, Angew. Chem., Int. Ed., 2015, 54, 8777.

5 J. Mayans, M. Font-Bardia and A. Escuer, Dalton Trans., 2018, 47, 8392.

6 L. A. Kushch, A. V. Nikolaev, E. B. Yagubskii, S. V. Simonov, R. P. Shibaeva, A. V. Sadakov, O. E. Omel'yanovskii and V. S. Mironov, Inorg. Chem. Commun., 2012, 21, 57.

7 K. Mason, A. Prescimone, M. Schau-Magnussen, S. Piligkos, P. A. Tasker and E. K. Brechin, Curr. Inorg. Chem., 2013, 3, 76.

8 T. Taguchi, T. C. Stamatatos, K. A. Abboud, C. M. Jones, K. M. Poole, T. A. O'Brien and G. Christou, Inorg. Chem., 2008, 47, 4095.

9 E. K. Brechin, M. J. Knapp, J. C. Huffman, D. N. Hendrickson and G. Christou, Inorg. Chim. Acta, 2000, 297, 389.

10 C. A. Christmas, H.-L. Tsai, L. Pardi, J. M. Kesselman, P. K. Gantzel, R. K. Chadha, D. Gatteschi, D. F. Harvey and D. N. Hendrickson, J. Am. Chem. Soc., 1993, 115, 12483.

11 W. Wang, B. Spingler and R. Alberto, Inorg. Chim. Acta, 2003, 355, 386.

12 K. C. Mondal, O. Sengupta and P. S. Mukherjee, Inorg. Chem. Commun., 2009, 12, 682.

13 V. Bertolasi, G. Annibale, G. Marangoni, G. Paolucci and B. Pitteri, J. Coord. Chem., 2003, 56, 397.

14 A. Ch. Kalita, S. K. Gupta and R. Murugavel, Chem. – Eur. J., 2016, 22, 6863.

15 M. G. B. Drew, S. Nag, P. K. Pal and D. Datta, Inorg. Chim. Acta, 2008, 361, 2562.

16 A. M. Guidote Jr., K. Ando, Y. Kurusu, H. Nagao and Y. Masuyama, Inorg. Chim. Acta, 2001, 314, 27.

17 P. Dhal, A. Sasmal, C. J. Gómez-García, A. Bauzá, A. Frontera, G. Pilet and S. Mitra, Eur. J. Inorg. Chem., 2014, 3271.

18 M. Enamullah, A. C. Chamayou, K. S. Banu, A. C. Kautz and C. Janiak, Inorg. Chim. Acta, 2017, 464, 186.

19 D. Pijper, P. Saisaha, J. W. de Boer, R. Hoen, C. Smit, A. Meetsma, R. Hage, R. P. van Summeren, P. L. Alsters, B. L. Feringa and W. R. Browne, Dalton Trans., 2010, 39, 10375.

20 G. Abbas, M. Ibrahim, S. F. M. Schmidt, E. Moreno-Pineda, C. E. Anson and A. K. Powell, Polyhedron, 2019, 158, 255.

21 O. A. Adebayo, K. A. Abboud and G. Christou, Polyhedron, 2017, 122, 71.

22 C. A. Grapperhaus, M. G. O'Toole and M. S. Mashuta, Inorg. Chem. Commun., 2006, 9, 1204.

23 J. Burger and P. Klüfers, Angew. Chem., Int. Ed. Engl., 1991, 36, 776.

24 G. E. Kostakis, V. A. Blatov and D. M. Proserpio, Dalton Trans., 2012, 41, 4634.

25 V. A. Blatov, IUCr CompComm. Newsletter, 2006, 7, 4.

26 S. M. Gorum and S. J. Lippard, Inorg. Chem., 1991, 30, 1625.

27 H. Weihe and H. U. Güdel, J. Am. Chem. Soc., 1997, 119, 6539.

28 K. J. Mitchell, K. A. Abboud and G. Christou, Inorg. Chem., 2016, 55, 6597.

Legends to figures

Scheme 1. R-MeO-hpm− ligand found in complexes 1–3. Asterisks denote the chiral C-atoms. Its origin can be from hydrolysis of L1 or the direct reaction of the intermediate reagents.

Figure.1 Left, view of the molecular structure of complex 2. Right, common {Fe10O16} core for clusters 1–3. The labeled core for 3 is shown in Fig. S4.†.

Figure.2 Core of complexes 1–3 showing the different coordination environment for Fe2 and Fe6 and the H-bonds between the monodentate nitrates and the μ3-OH donors.

Scheme 2 The two different distortions of J15 which result in the conventional J17 dodecahedron (left) or in the new polyhedron of clusters 1–3 (right). Center, Fe10 metallic core of complexes 1–3 and a view of the unprecedented {M10(μ3-O)8} fragment (the orange bold edges enhance the distorted inner cube).

Figure.3. Susceptibility vs. temperature product for complexes 1–3. Inset, χM plot for complex 2, showing the susceptibility maximum at 6 K.

Figure.4 Left, core of complex 1 showing the MSC predicted J values. Right, derived spin alignment rationalizing its S = 0 ground state.

SCHEME 1

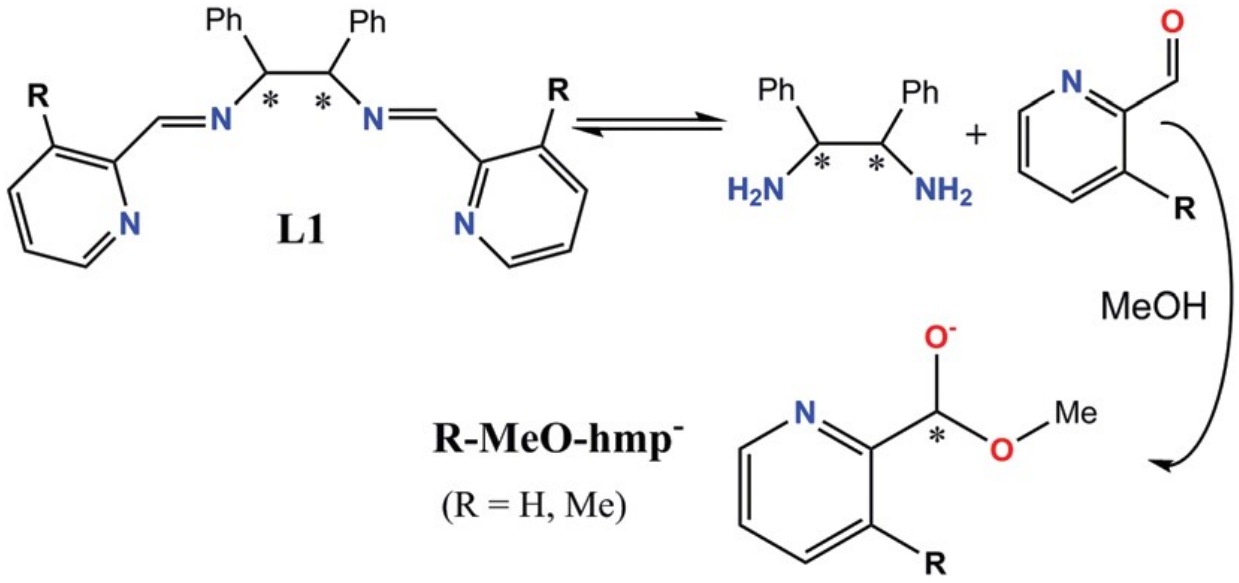

FIGURE 1

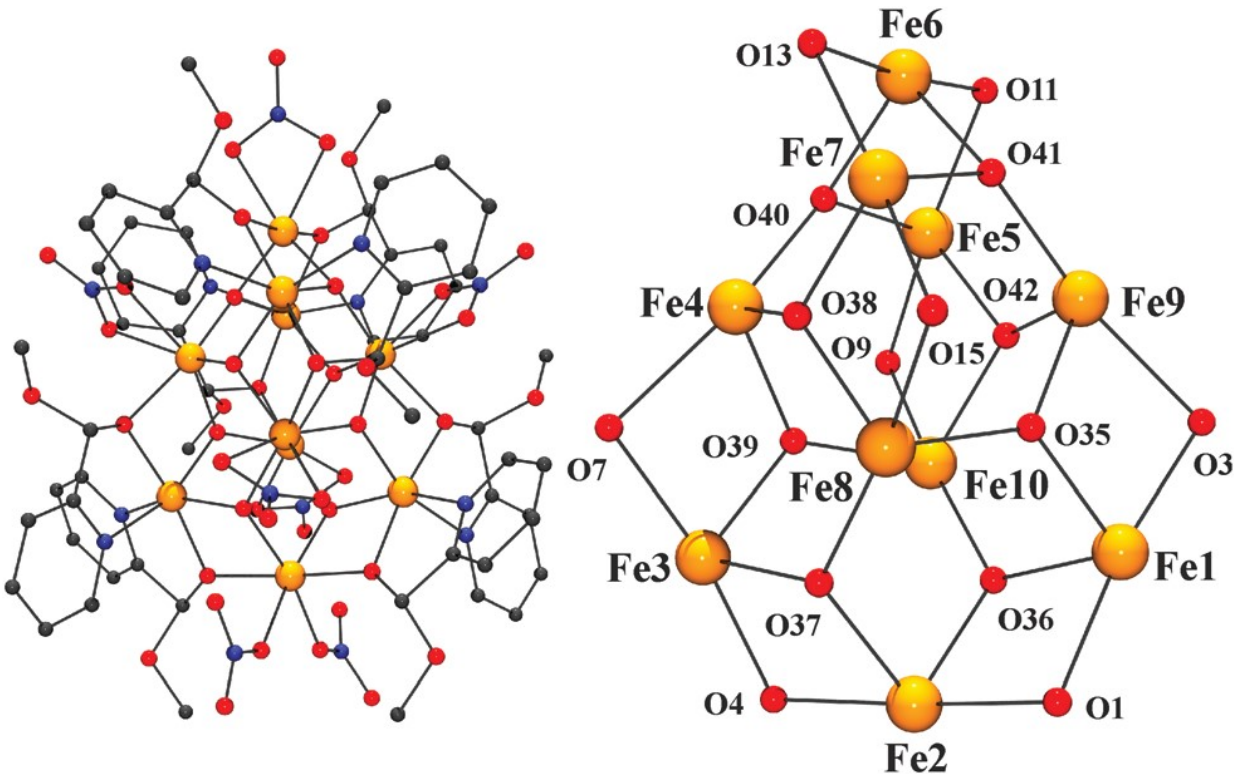
Fe6
O13
O11
Fe7
O41
O40
Fe5
Fe4
O38
O42
Fe9
O9
O15
O7
O39
O35
O3
Fe8
Fe10
Fe3
Fe1
O37
O36
O4
O1
Fe2

FIGURE 2

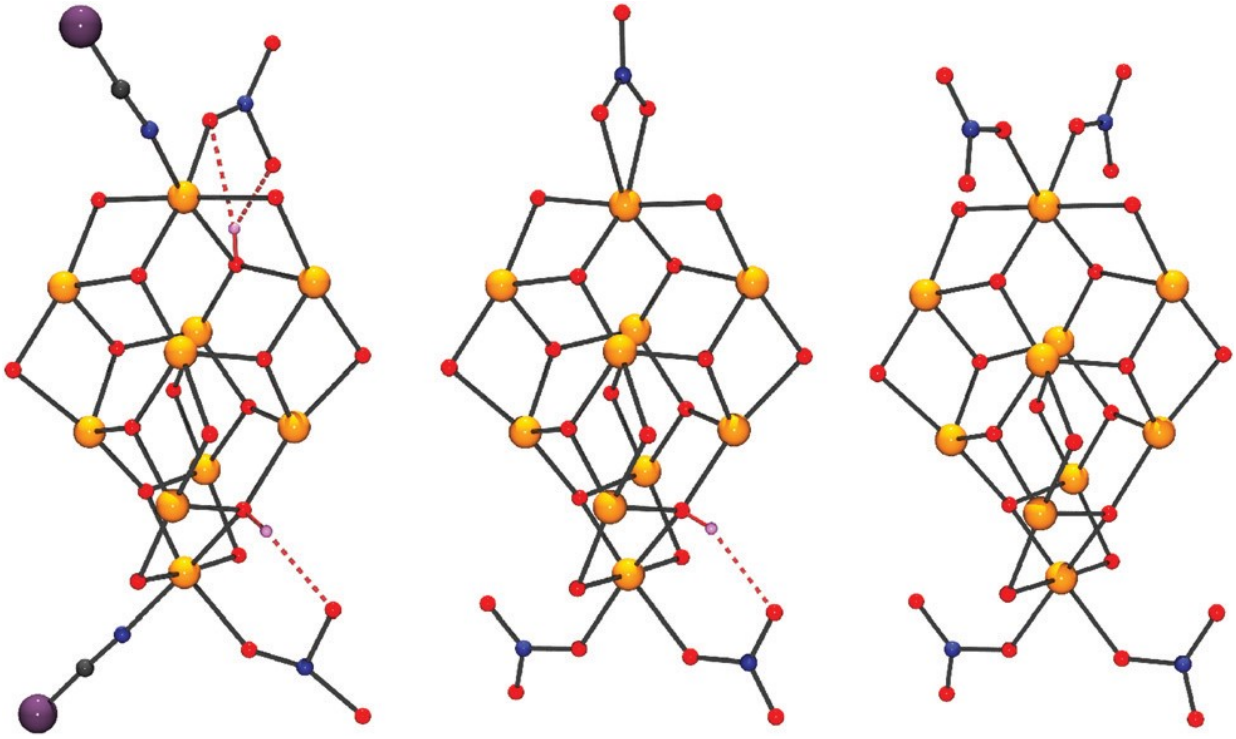

SCHEME 2

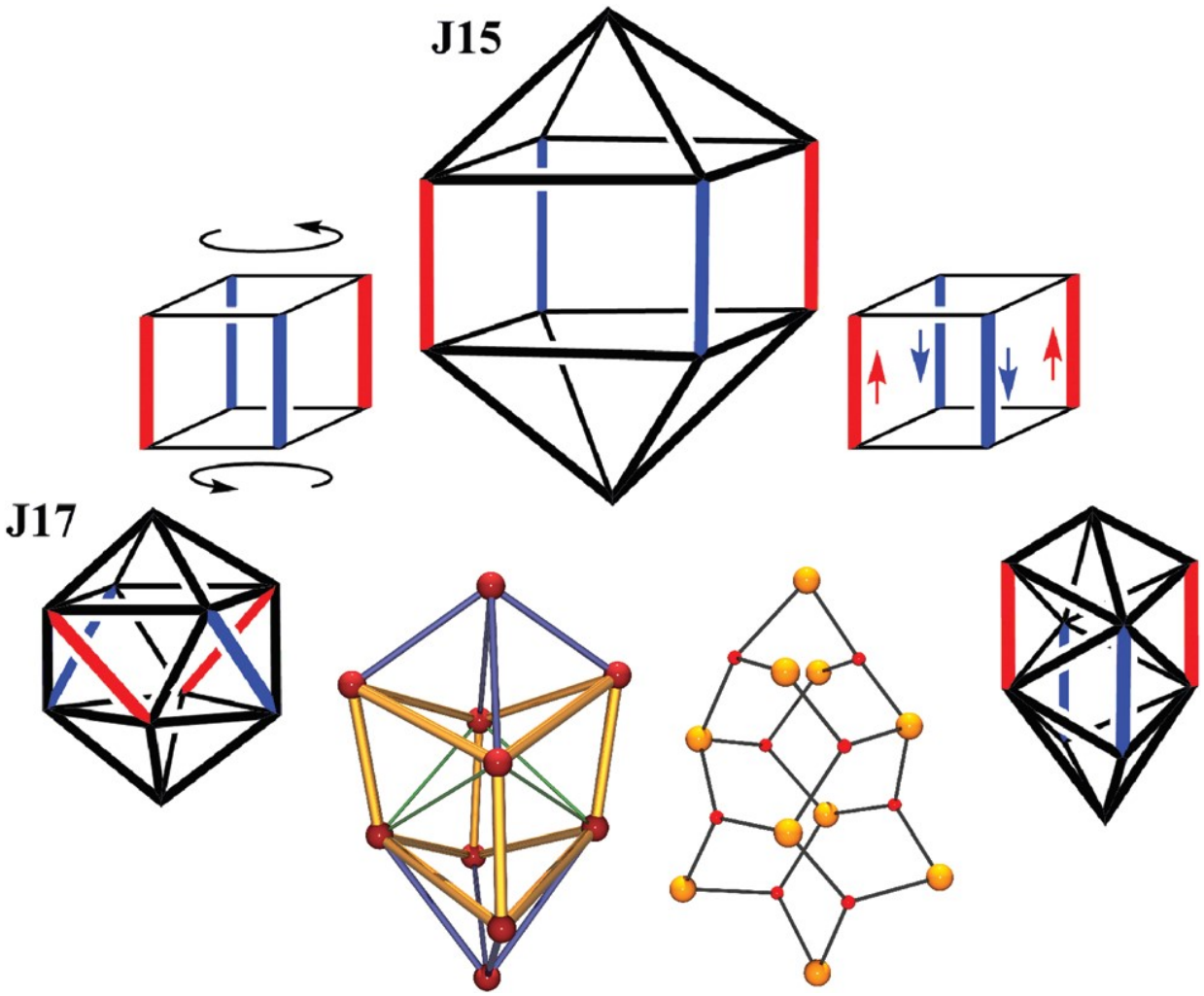

253 **FIGURE 3**

254

255

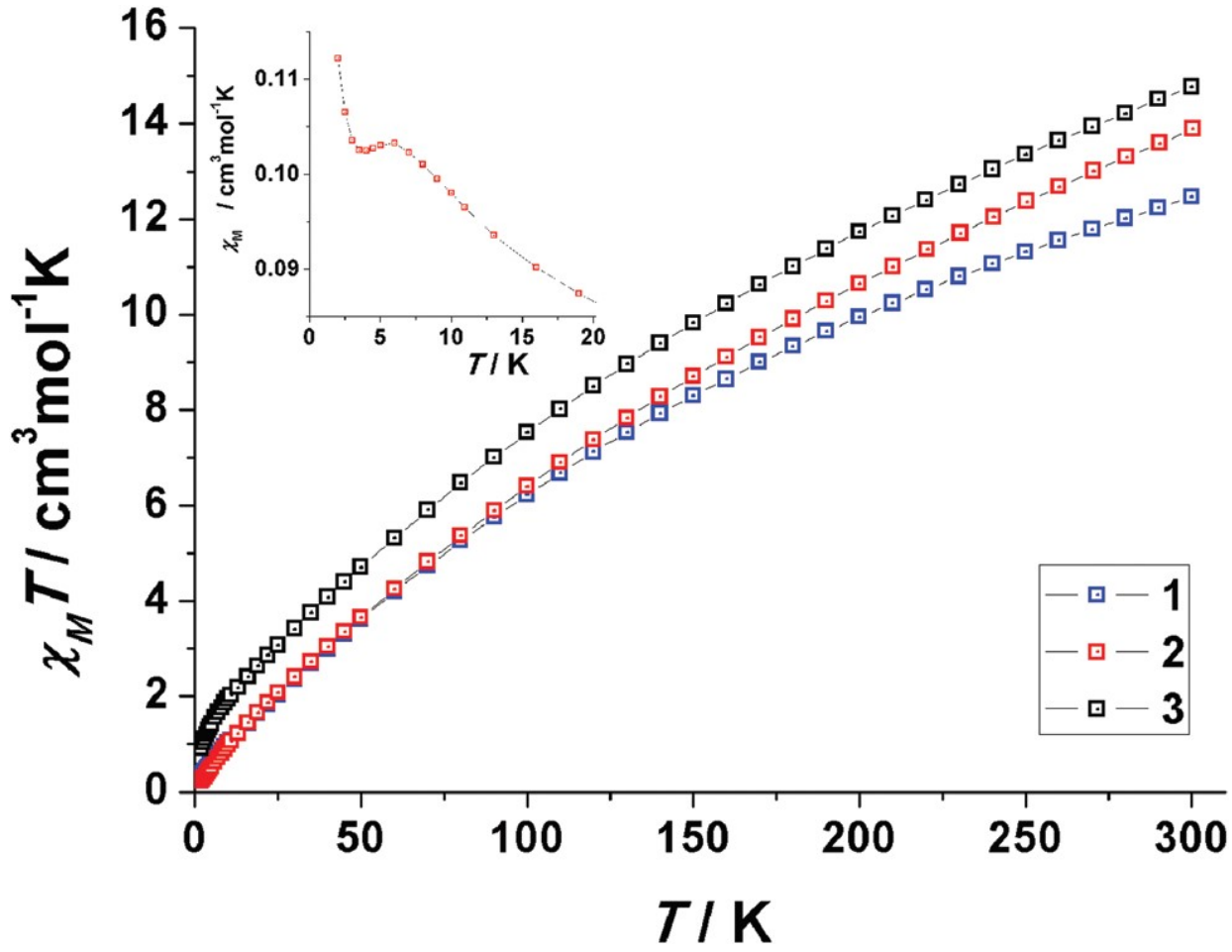

256

257

FIGURE 4